

AFORS-HET: A COMPUTER-PROGRAM FOR THE SIMULATION OF HETEROJUNCTION SOLAR CELLS TO BE DISTRIBUTED FOR PUBLIC USE

A. Froitzheim¹, R. Stangl, L. Elstner, M. Kriegel, W. Fuhs

Hahn-Meitner-Institut Berlin, Abt. Silizium-Photovoltaik, Kekuléstr. 5, D-12489 Berlin, Germany.

¹Corresponding author: froitzheim@hmi.de

ABSTRACT

We offer a numerical simulation tool, AFORS-HET, for public use, which allows to model homo- as well as heterojunction devices. AFORS-HET is the short form of **automat for simulation of heterostructures** and can be downloaded via the internet: <http://www.hmi.de/bereiche/SE/SE1/projects/aSiSi/AFORS-HET>

An arbitrary sequence of semiconducting layers can be modelled. A variety of boundary conditions can be chosen. The program solves the one dimensional semiconductor equations in steady-state and for a small sinusoidal ac-perturbations. Furthermore, a variety of common characterisation techniques have been implemented, like current-voltage (IV), internal quantum efficiency (IQE), impedance, capacitance (CV, CT), static surface photovoltage (SPV), electron beam induced current (EBIC) and photoluminescence (PL). A user-friendly interface allows to easily perform parameter variations, and to visualise and compare your simulations.

1. INTRODUCTION

In order to investigate amorphous/crystalline silicon heterojunctions a lot of different electrical measurement methods have been used, as high efficiencies have been reached [1]. Besides standard solar cell characterisation techniques, such as current-voltage (I-V) and internal quantum efficiency (IQE), more advanced characterisation techniques have been applied, like capacity-voltage (C-V) [2], photoluminescence (PL) [3], or electroluminescence (EL) [4]. We therefore developed a numerical simulation tool, which allows to simulate the output of all these measurement techniques for hetero structures consisting of ultra thin a-Si:H layers (5 nm) combined with thick c-Si layers (300 μm). We extended the capability of the program in the sense that now an arbitrary sequence of semiconducting layers and interfaces with an arbitrary number of defects distributed within the band gaps can be simulated, being able to choose among different models for the transport of charge carriers across the interfaces. Furthermore, we introduced a user friendly interface, which allows to perform multidimensional parameter variations and to easily visualise and analyse the corresponding results.

2. PHYSICAL MODEL

2.1 Bulk

The steady state of the heterostructure is modelled by the use of the semiconductor equations [5, p.9]:

$$\frac{\partial D}{\partial x} = +q(p - n + \rho + N_D - N_A) \quad (1)$$

$$\frac{\partial J_n}{\partial x} = -q(G - R_n) \quad (2)$$

$$\frac{\partial J_p}{\partial x} = +q(G - R_p) \quad (3)$$

Here, D is the displacement field, p and n the hole and electron densities, ρ is the net charge of all traps located in the band gap, $N_{A/D}$ is the acceptor and donor concentration, respectively. J_n and J_p are the electron and hole current densities, G the optical generation Rate, R_n and R_p are the electron and hole recombination rates. The recombination is modelled by auger-, direct band to band-, and Shockley-Read-Hall recombination. We used boltzmann statistics for the calculation of electron as well as hole concentration.

2.2 Boundary conditions

The potential is fixed to zero at the front contact. It is determined by the sum of the difference of the metal contact work functions at the front and rear contact and the applied voltage at the rear contact if voltage controlled boundary conditions are chosen. The electron and hole currents into the metal contacts are modelled by thermionic emission. At the front contact ($x=0$) the equations.

$$\varphi(0) = 0 \quad (4)$$

$$J_n(0) = +q \cdot S_n^f (n(0) - n_{eq}(0)) \quad (5)$$

$$J_p(0) = -q \cdot S_n^f (p(0) - p_{eq}(0)) \quad (6)$$

are applied. The algebraic signs of eq. (5) and (6) account for the projection of the direction vector of current density to the normal vector of the front surface. At the rear contact ($x=w$), with an applied voltage V the equations

$$\varphi(w) = \phi_f - \phi_b - V \quad (7)$$

$$J_n(w) = -q \cdot S_n^b (n(w) - n_{eq}(w)) \quad (8)$$

$$J_p(w) = +q \cdot S_n^b (p(w) - p_{eq}(w)) \quad (9)$$

have to be fulfilled. ϕ_f and ϕ_b are the metal work functions of the front and rear contact, respectively. S is the recombination velocity at the specified contact. For majority carriers S is usually the thermal velocity of the corresponding charge carriers. For minority carriers S can be much smaller, depending on the surface passivation.

Other boundary conditions could be used as well: If current controlled boundary conditions are used, eq. (7) is replaced by an equation which says that the applied current is equal to be the sum of the electron and hole current. An other possibility is to use insulating boundary conditions. In this case it is assumed that the electron and hole current has to recombine at the insulating interfaces and no net current crosses the Insulator. For the boundary condition of the potential Gauß's law is applied and eq. (7) is replaced by:

$$\varepsilon_{sem} \frac{\partial \varphi}{\partial x} \Big|_{sem} - \varepsilon_{ins} \frac{\partial \varphi}{\partial x} \Big|_{ins} - Q_{int} = 0 \quad (10)$$

ε_{sem} and ε_{ins} is the permittivity in the semiconductor and the insulator respectively. Q_{int} represents the the charge at the interface. If the user wants to use this boundary condition he has to adjust the Capacitance and thickness of the insulating layer and has to chose MIS boundary conditions.

2.3 Interfaces

The interfaces can be modelled in two ways:

(a) No additional boundary conditions are applied, but the current of the holes is modelled by modified expressions for the currents, which account for the fact, that currents are additionally driven by gradients in the effective densities of state as well as gradients in the energy gap and electron affinity. This approach is equal to the approach of the simulation tool AMPS 1D [6].

(b) themionic emission model, fig. 1: This model is also used in SCAPS 1D [7] and uses the model from Pauwels formalism [8] for recombination currents across the interfaces. The transport of

charge carriers from one semiconductor to the other is modelled via thermionic emission and by recombination across interface

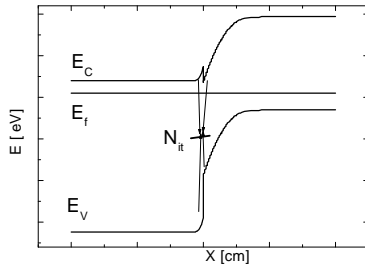


Fig. 1: Recombination model for the simulation of recombination after [8]. Interfacestates N_{it} interact mit both adjacent semiconductors and thus for recombination paths are indicated.

defect states. This states interact not only with one but with both adjacent semiconductors. Therefore charge carriers can transverse the interface via defect states from one semiconductor to the other. As a consequence the distribution function of the defect is modelled by four capture cross-sections, two for the holes and two for the electrons in the adjoining two semiconductors. The potential is

assumed to be continuous across the interface. Therefore this model excludes the modelling of buffer layers, that only act as dipole

3. NUMERICAL PROCEDURES

AFORS-HET solves the semiconductor equations (1)-(3) and the appropriate boundary conditions in one dimension numerically. The set of coupled partial differential equations is transformed into a set of nonlinear algebraic equations by the method of finite differences. The electron and hole currents are discretised by an exponential fitting scheme in order to enhance numerical accuracy and convergence [5, p. 157]. The resulting set of equations have to be solved on a lattice, which represents the continuum of the differential equations as well as possible. We used n_1 , p_1 and φ_1 at each lattice point as independent variables. All other variables, e. g. R_n , R_p depend on n , p and φ . The three equations (1)-(3) and the boundary conditions for the rear and front contact can be viewed as a three dimensional vector $\mathbf{G}_1(n,p,\varphi)$, with one dimension for each equation. The set of N vectors \mathbf{G}_1 have to be fulfilled at the N lattice points of the discretisation scheme and can be written as

$$G_i = 0, \forall i \quad (11)$$

The calculation of n , p and φ is done by an iteration scheme which needs a well adopted guess for these variables. The calculation of this guess will be explained now and will also show where the lattice points of the discretisation are placed.

First the Charge neutrality is calculated for each layer, giving n and p in each lattice point of the layer. With the knowledge of the charge carrier concentration, the electron affinities and the doping concentrations, the voltage drops in each layer can be calculated from analytical models [9, p. 76]. Assuming a x^2 dependence of the potential from distance in space charge regions a first suggestion is given for the potential. The lattice points, on which the algebraic semiconductor equations have to be solved, are set equally distanced in a user defined potential spacing, not in distance spacing. The lattice points in the neutral regions have the same distance from each other. Altogether the lattice points are adjusted in a way that there are a lot of lattice points within the space charge regions and viewer points are within the neutral regions. It should be mentioned, that the lattice spacing is not optimised to the absorption coefficient of the layer. This might result in bad approximation for the exponential decaying generation rates if the sample is illuminated. The lattice points are fixed during calculation.

The solution of the semiconductor equations is found by the Newton Raphson iteration algorithms [5, p. 208]: The $k+1$ solution of \mathbf{G}_1^{k+1} is found from the previous solution \mathbf{G}_1^k with the help of a correction vector which is calculated from the Jacobimatrix of \mathbf{G} . This procedure is recalculated until a desired accuracy c is reached:

$$abs(|G_i|) < c, \forall i \quad (12)$$

c has to be adopted by the user. We solve for the new n_1 , p_1 , and φ_1 in one step by calculating all three semiconductor equations in one step and not by solving each of the 3 semiconductor equations step by step with new calculation of p after n after φ , as it is done by the Gummel algorithm. This procedure gives better convergence

for the modelling of defect rich materials such as a-Si:H, as the

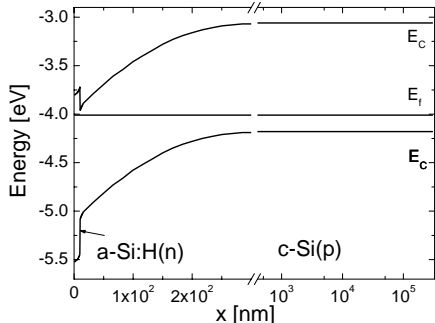


Fig.2: simulated band diagrams at equilibrium of a-Si:H(n)/c-Si(p) as it is used in reference [12]. The a-Si:H(n) layer thickness is 10 nm in this calculation.

coupling of the semiconductor is enhanced if high defect densities with high recombination rates are involved.

No special equations have been used to solve the semiconductor equations for thermal equilibrium. The boundary conditions are adjusted to $V = 0V$, and naturally, no illumination is applied. For steady state the desired boundary conditions have to be chosen, e.g. voltage or current and monochromatic and/or spectral illumination. Please note, that the solution to the new boundary conditions are calculated from the last solution. So, if a calculation fails it might be a good idea to adjust the new boundary conditions step by step to the desired values.

Once the steady state solution is found the ac-solution is calculated in one step by a linear expansion of the semiconductor equations, which result in [10]:

$$\frac{\partial \tilde{D}}{\partial x} = +q(\tilde{p} - \tilde{n} + \tilde{\rho}) \quad (13)$$

$$\frac{\partial \tilde{J}_n}{\partial x} = -q(\tilde{G} - \tilde{R}_n - i\omega \cdot \tilde{n}) \quad (14)$$

$$\frac{\partial \tilde{J}_p}{\partial x} = +q(\tilde{G} - \tilde{R}_p - i\omega \cdot \tilde{p}), \quad (15)$$

where the tilde \sim indicates a small signal complex amplitude, j is the imaginary unit. By definition the system is linear in the small signal amplitudes of n , p and ϕ , the system can easily be solved by inverting a complex Jacobimatrix just once. In the ac-Mode it is assumed, that the steady state solution is already found, thus \mathbf{G}_1 is equal to zero for all lattice points and the small signal amplitude of the disturbance has to be added to each lattice point. For example if a small ac-voltage is applied at the rear contact the small signal perturbation is only at the last lattice point. If a modulated light source is used as small signal ac perturbation, every lattice point is disturbed. More detailed information concerning the physical model and the algebra behind can be found in [11] and references therein.

4. SELECTED RESULTS

In the following section we like to give a short overview of the capabilities of the program. We used the tool so far mainly to simulate amorphous/crystalline silicon heterojunction solar cells.

4.1 Simulation of band diagrams:

After having input the layer structure the thermodynamic equilibrium is solved for this heterojunction. Band diagrams, current densities, charge carrier concentrations are presented in a separate window. As an example, the band diagram of a typical a-Si:H/c-Si structure is presented in fig. 2.

The graphs can be modified according to the users wishes, e.g. log or linear scale, zooming, defining a certain range and more. Also some mathematical operations can be done directly in this window, such as measuring values, differences of two specified points or the integral of a certain range can be evaluated.

4.2 Applying measurements

After the thermodynamic equilibrium is calculated for the structure the steady state measurement methods current voltage (IU), quantum efficiency (IQE), electron beam induced current (EBIC), surface photo voltage (SPV voltage, SPV spectral), and the small signal ac- methods Admittance, Impedance, capacity voltage (CV), capacity temperature (CT) can be applied with and without illumination. For illumination either a special spectrum and or monochromatic illumination can be used or a file that contains the generation profile can be loaded. Furthermore Sub-bandgap photon absorption can be simulated by specification of optical capture cross sections. As an example The quantum efficiency of a a-Si:H(n)/c-Si is shown in figure 2 for a-Si:H(n) emitter thickness from 2 to 20 nm.

As can be seen in the figure, absorption and reflection files can directly be included in the calculation. The thinner the defect-rich a-Si:H(n) emitter can be deposited, the less electron-hole pairs created in the emitter will recombine. Thus the internal quantum efficiency between 300 nm and 650 nm will be significantly enhanced by using ultra thin a-Si:H emitters.

As an example for an simulation where small signal method is used a CV simulation is shown in fig. 3. From this graph it is possible to recalculate the doping concentration [9, p. 80] giving a doping concentration of $1.5e16 \text{ cm}^{-3}$ and $5e15 \text{ cm}^{-3}$, respectively as they have been input in the modelling of c-Si(p). The CV plot shows also simulation for various built in voltages by changing the band offset at the heterojunction interface. The calculated built in voltage from this graph correspond to the analytical values as long as the fermilevel does not touch the conduction band edge.

As a last example the photoluminescence of an illuminated cell at open circuit condition is shown for two defect concentrations at the a-Si:H/c-Si interface.

The spectrum is calculated from a generalised Planck's law that takes the splitting of the quasi fermilevels and the absorption coefficients of the materials into account [Würfel]. The PL signal is very sensitive to Defect concentrations as this will reduce the charge carrier concentration at open circuit conditions that determine the splitting of the quasi fermi level. This method could be used to simulate electroluminescence measurement methods as well, only the appropriate boundary conditions have to be applied.

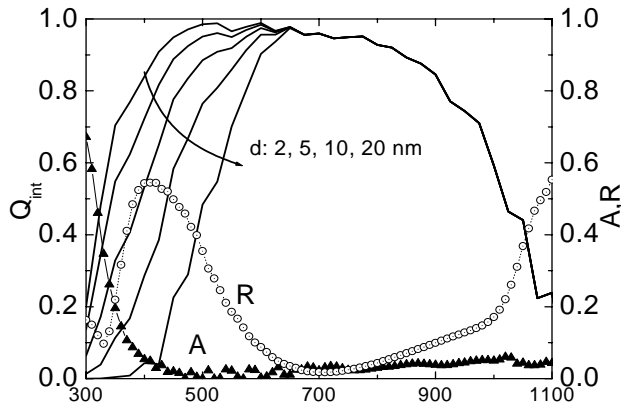


Fig 3: Simulated internal quantum efficiency of TCO/a-Si:H(n)/c-Si(p) solar cells with varying emitter thickness. The TCO front contact absorption A and the reflection R, which has been used as an input parameter within the simulation, is also shown.

A very interesting feature of AFORS-HET is the ability to do parameter variations automatically. This feature is easy to handle if one tries it a little bit, but far more complicated to explain. We encourage you to use the program and to try it by your own.

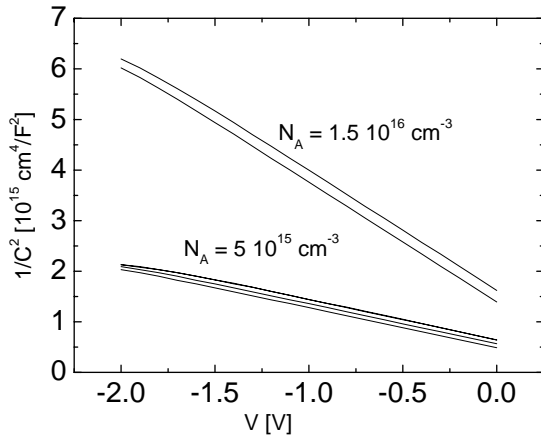


Fig.4: Simulated CV measurements for two doping concentrations N_A and various band offsets, resulting in differing built-in voltages.

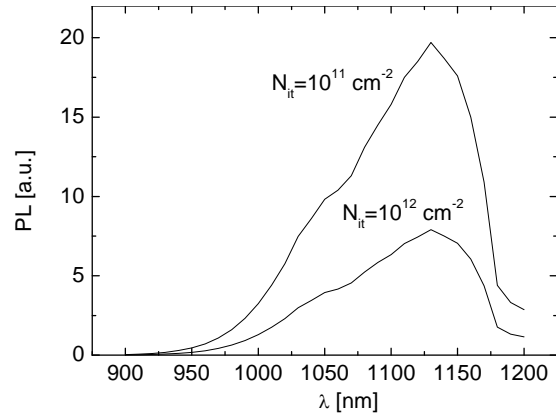


Fig. 5: Photoluminescence spectra at open circuit conditions for two densities of defect states N_{it} . The spectra has its maximum around the band gap energy of c-Si.

4. CONCLUSION AND OUTLOOK

A new simulation tool has been presented: AFORS-HET. It runs on PC with Window 98, Window NT and more recent versions. If there is a high interest we will also try to run AFORS-HET on LINUX systems. Originally it was planned that we want to distribute AFORS-HET as open source code, but we think the code is not well enough documented and it is not strictly enough programmed in OOP. However, if there is a huge interest, we will try to manage it. Any updates and news can be found on the webpage given in the abstract. Do not hesitate contacting us in case of questions or comments.

References

- [1] H.Sakata, T.Nakai, T.Baba, M.Taguchi, S.Tsuge, K.Uchihashi, S.Kiyama, *Proc. 28th IEEE PVSEC* (2000), 7.
- [2] N. Jensen, R.M. Hsusner, R.B. Bergmann, J.H. Werner, U. Rau, *Prg. In PV: Res. A. Appl*,
- [3] G.H. Bauer, K. Bothe, T. Unold, *28th IEEE PVSEC*(2002), 700.
- [4] M.S. Bresler, O.B. Gusev, E.I. Terukov, A. Froitzheim, W. Fuhs, A. Gudovskikh, J.P. Kleider, Terukov
- [5] Selberherr, *Analysis and simulation of semiconductor devices*, Springer Wien, 1984.
- [6] AmPS!D
- [7] A. Niemegeers, S. Gillis, M. Brugelman, *Proc. 2nd World PVSEC* (1998), 674.
- [8] H. Pauwels, G. Vanhoutte, *J. Phys. D: Appl. Phys.*, **11** (1978), 2079.
- [9] S.M. Sze, *Physics of Semiconductor Devices*, John Willey and Sons, 1981.
- [10] S. Laux, *IEEE Trans. ED*, **32** (1985), 2078.
- [11] A. Froitzheim, PHD-Thesis, not yet available.
- [12] R. Stangl, A. Froitzheim, M. Schmidt, W. Fuhs, this Concurrence.